*The 2018 Structures Congress (Structures18)*
*Songdo Convensia, Incheon, Korea, August 27 - 31, 2018*

# Numerical Analysis of Response of T-Shaped RC Shear Walls under Biaxial Loading

*Ting-Wei Chang[1)] and Chung-Chan Hung [2)]

*[1), 2)] Department of Civil Engineering, National Cheng Kung University, Taiwan.*
*[1)] no0963035974@gmail.com*

## ABSTRACT

Nowadays one of the techniques to increase the lateral load capacity and structural stiffness of high-rise buildings is by using Reinforced concrete (RC) structural walls. According to former researchers, the lateral load capacity of the structural walls is influenced by the interaction between its weak and strong axis. In this study, it was done a pushover analysis to comprehend the behavior of T-shaped RC walls under biaxial loading.

LS-DYNA was used to simulate different scenarios in which the model had out-of-plane deflections on the weak axis with drift ratios of 1%, 2%, 4%. Then a monotonic load of % was included on the strong axis. It was possible to realize a comparison between the response of uniaxial and biaxial loading.

The results indicate that a major factor on the behavior of T-shaped wall subjected to biaxial loading was the tension in the flange. It was observed that the increase in the axial load significantly decreased the lateral load capacity. On the other hand, an increase in the width of the flange only caused minor decrease in lateral load capacity.

## 1. INTRODUCTION

The lateral load capacity and structural stiffness of high-rise buildings can be improved by including Reinforced concrete (RC) structural walls in the structural design. Previous studies have tried to explain interaction between the strong and weak axis of RC walls and its influence on the lateral load capacity. A modeling simulation was done using the pushover analysis of T-shaped RC walls subjected to biaxial loading and considering the shear lag effect on the flange.

## 2. METHODS

---

[1)] Graduate Student
[2)] Professor

LS-DYNA was the software used to analyze the pushover on RC Walls. The materials and elements used are described below.

### 2.1. Material Model

#### 2.1.1. Concrete: Continuous Surface Cap Model

For this study, Material type 159 (MAT_CSCM_CONCRETE) was the concrete model used with solid elements. It is very popular in modeling concrete structures because it allows capturing damage parameters and concrete characteristics. The continuous surface cap model is composed of a shear failure surface and a hardening surface cap (see Fig. 2.1). The parameters are shown in Table 2.1.

#### 2.1.2. Steel Reinforcement: Kinematic Hardening Plasticity Model

To obtain the kinematic hardening plasticity, the Material type 3 (MAT_PLASTIC_KINEMATIC) was used to model the reinforcement material of the beam elements. By using this type of element, it is possible to define the Young's modulus and the tangent modulus by creating a bilinear curve (see Fig.2.2). The parameters are shown in Table2.2.

Table2.1 Concrete Material Parameters

| *MAT_CSCM_CONCRETE_TITLE | | | | | | | | | | |
|---|---|---|---|---|---|---|---|---|---|---|
| ro | nplot | incre | irate | erode | recov | itretrc | pred | fpc | dagg | units |
| 2.4E-5 | 1 | 0 | 0 | 1.05 | 0 | 0 | 0 | 31.7 | 0 | 2 |

Table2.2 Reinforcement Material Parameters

| *MAT_PLASTIC_KINEMATIC_TITLE | | | | | | | | | |
|---|---|---|---|---|---|---|---|---|---|
| ro | e | pr | sigy | etan | beta | src | srp | fs | vp |
| 7.83E-5 | 200000 | 0.28 | 550 | 0 | 0 | 0 | 0 | 0 | 0 |

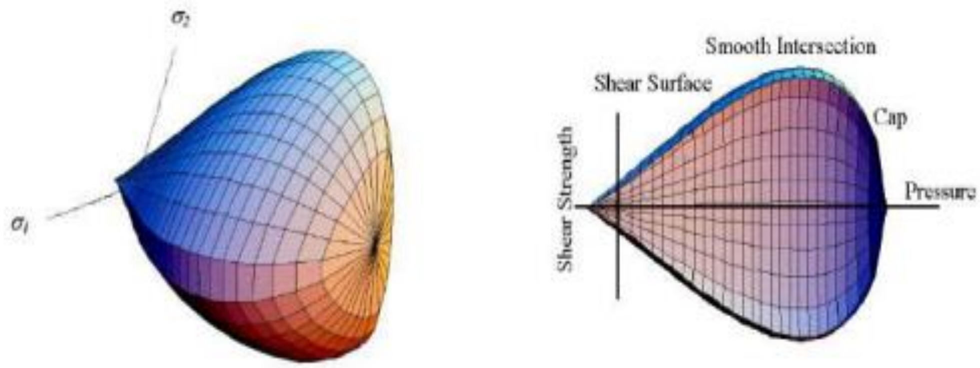


Fig.2.1 General shape of the concrete model yield surface

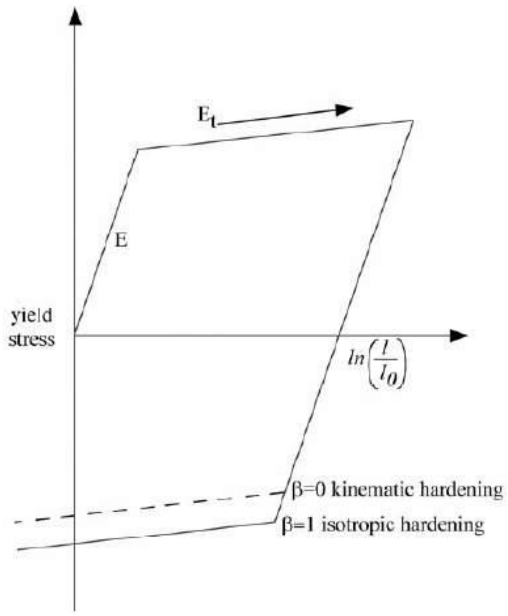


Fig.2.2 Elastic-plastic behavior of material type 3 (Krieg and Key, 1976)

## 2.2.Geometry and Boundary Conditions

For the parametric study, 108 specimens were modeled. All the specimens had a thickness of the web of 300 mm and the flange of 2400 mm. Three flange width were used: 1260 mm, 2340 mm, and 3660 mm. To idealize different types of walls, the three heights were used: 1200 mm, 3600 mm, and 7200 mm. The corresponding aspect ratios of the shear walls were of 0.5, 1.5 and 3.0 and at the top of the specimens, which were under compression; three different axial load ratios were applied: 0, 0.10 and 0.20. Details of the geometry are presented in Fig.2.3, Table2.3 and Table2.4.

Table2.3 Details of Wall Specimens for Validation (1)

| Model Types | Aspect ratio (a/d) | $f_c'$(MPa) | $f_y$(MPa) | $b_f$(mm) | $t_f$(mm) | $b_w$(mm) | $t_w$(mm) |
|---|---|---|---|---|---|---|---|
| T1W1L | 0.5 | 40 | 420 | 2340 | 300 | 2400 | 300 |
| T1W1M | 1.5 | 40 | 420 | 2340 | 300 | 2400 | 300 |
| T1W1H | 3.0 | 40 | 420 | 2340 | 300 | 2400 | 300 |
| T1W2L | 0.5 | 40 | 420 | 3660 | 300 | 2400 | 300 |
| T1W2M | 1.5 | 40 | 420 | 3660 | 300 | 2400 | 300 |
| T1W2H | 3.0 | 40 | 420 | 3660 | 300 | 2400 | 300 |
| T1W3L | 0.5 | 40 | 420 | 1260 | 300 | 2400 | 300 |
| T1W3M | 1.5 | 40 | 420 | 1260 | 300 | 2400 | 300 |
| T1W3H | 3.0 | 40 | 420 | 1260 | 300 | 2400 | 300 |

$f_c'$ : Compressive strength of concrete.
$f_y$ : Yield stress of reinforcing steel.
$b_f$ : Flange width of shear walls.
$t_f$ : Flange thickness of shear walls.
$b_w$ : Web width of shear walls.
$t_w$ : Web thickness of shear walls.

Table2.4 Details of Wall Specimens for Validation (2)

| Model Types | $\rho_{fl}$ | $\rho_{ft}$ | $\rho_{fbl}$ | $\rho_{wl}$ | $\rho_{wt}$ | $\rho_{wbl}$ | $\rho_{fs}$ | $\rho_{ws}$ | s (mm) |
|---|---|---|---|---|---|---|---|---|---|
| T1W1L | 1% | 1% | 4% | 1% | 1% | 4% | 4% | 4% | 60 |
| T1W1M | 1% | 1% | 4% | 1% | 1% | 4% | 4% | 4% | 60 |
| T1W1H | 1% | 1% | 4% | 1% | 1% | 4% | 4% | 4% | 60 |
| T1W2L | 1% | 1% | 4% | 1% | 1% | 4% | 4% | 4% | 60 |
| T1W2M | 1% | 1% | 4% | 1% | 1% | 4% | 4% | 4% | 60 |
| T1W2H | 1% | 1% | 4% | 1% | 1% | 4% | 4% | 4% | 60 |
| T1W3L | 1% | 1% | 4% | 1% | 1% | 4% | 4% | 4% | 60 |
| T1W3M | 1% | 1% | 4% | 1% | 1% | 4% | 4% | 4% | 60 |
| T1W3H | 1% | 1% | 4% | 1% | 1% | 4% | 4% | 4% | 60 |

$\rho_{fl}$ : Vertical reinforcement ratio in the flange of a wall.
$\rho_{ft}$ : Horizontal reinforcement ratio in the flange of a wall.
$\rho_{fbl}$ : Vertical reinforcement ratio in the boundary of flange.
$\rho_{wl}$ : Vertical reinforcement ratio in the web of a wall.
$\rho_{wt}$ : Horizontal reinforcement ratio in the web of a wall.
$\rho_{wbl}$ : Vertical reinforcement ratio in the boundary of web.
$\rho_{fs}$ : Ratio of distributed shear reinforcement in a plane. Perpendicular to the direction of the applied shear in the boundary of flange.
$\rho_{ws}$ : Ratio of distributed shear reinforcement in a plane. Perpendicular to the direction of the applied shear in the boundary of web.
s : Spacing of shear reinforcement.

### 2.3. Biaxial Loading Pattern

The simulations are carried out by first imposing the out-of-plane deflections on the weak axis (y-axis), with drift ratios of 1%, 2%, 4%. Then, a 5% monotonic load on the strong axis (x-axis) was applied with a loading rate of 0.75mm/s, illustrated in Figure2.4. The effect of biaxial pushover behavior was investigated, and compared to the uniaxial behavior.

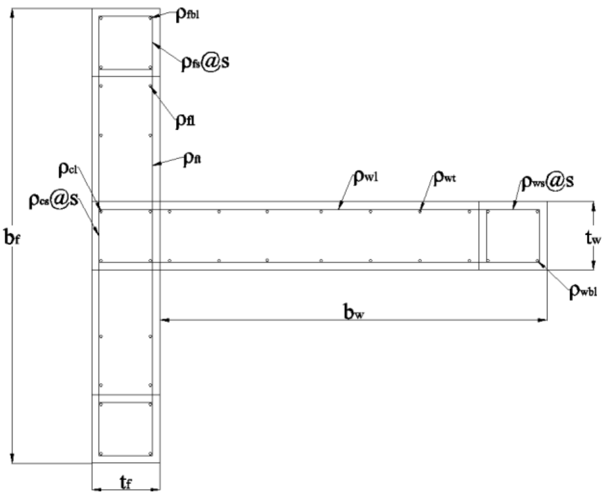


Figure2.3 Cross-section for the T-shaped walls

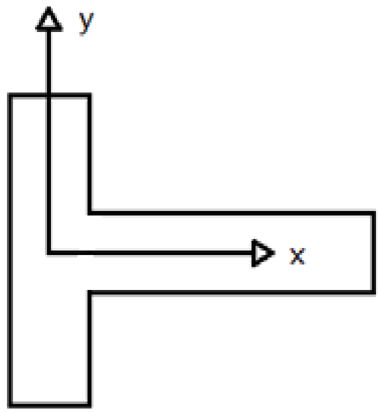


Figure2.4 Loading pattern applied on T-shaped walls

## 3. RESULTS

In this section, it is possible to observe the influence of different factors on the behavior of the T-shaped RC walls. The variables studied in the response pf the flange in tension stress are different aspect ratios, axial load ratios and T-shaped cross section, including crack pattern, damage progression, and the force displacement responses.

### 3.1 Crack Patterns

The plastic strain diagram shows the observed cracking patterns of the models at the final stage. According to the out-of-plane pushover, the lower part of the wall showed horizontal cracks in the middle of the web of the wall. The cracks in the flange were a mixture of horizontal and diagonal cracks, illustrated in Figure2.1(b), Figure2.2(b), Figure2.3(b). On the other hand, cracks were distributed over the web of the wall, induced by in-plane monotonic loading. The upper part of the wall featured diagonal cracks, induced by the shear force. The lower part of the wall showed diagonal cracks at the middle of the web of the wall. Also, the direction of the diagonal crack changed at the base of the wall and the angle increased with height. For the flange, cracks were only observed in the flange in the tension loading direction for both specimens. The cracks in the flange were a mixture of horizontal and diagonal cracks, illustrated in Figure2.1(c), Figure2.2(c), Figure2.3(c).

### 3.2 Ultimate Shear Strength

According to the results, the influence of biaxial displacements on the behavior of T-shaped walls was great when the flange was under tension. Figs.3.4 showed that the reduction of ultimate strength versus out-of-plane displacement with drift ratios of 1%, 2% and 4%. The increase in the axial load significantly decreased the lateral load capacity. Whereas, the increase of flange width and flange thickness caused minor decrease in lateral load capacity.

## 4. CONCLUSIONS

This paper numerically investigated the behaviors of T-shaped RC shear walls with various aspect ratios under biaxial loading. The influence of out-of-plane displacement on the lateral load capacity was found to be substantial. Further simulations have been conducted by the authors and comprehensive results will be used for studying the shear lag effect for flanged shear walls in the case of biaxial loading in the future.

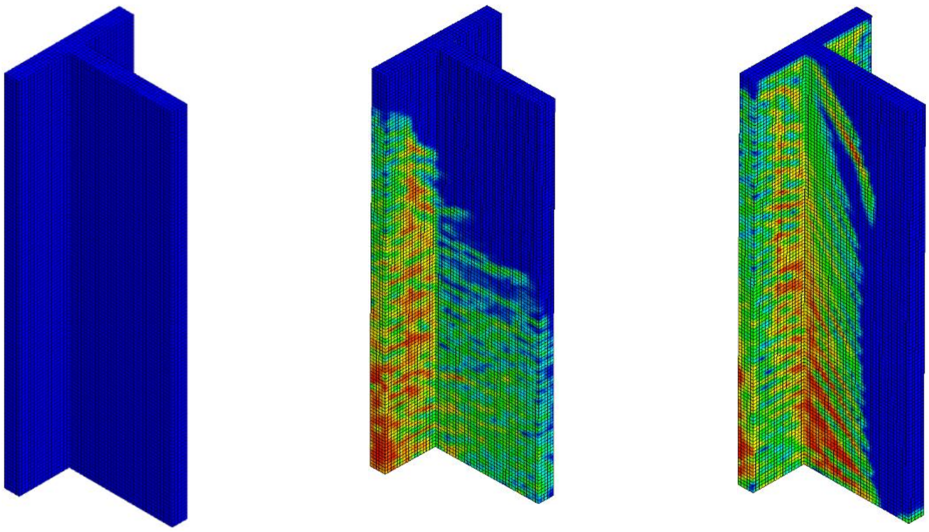

(a)Initial Condition (b)Out-of-Plane Pushover (c)In-Plane Pushover

Figure.3.1 Plastic Strain Diagram of Model of 3.0 Aspect Ratio

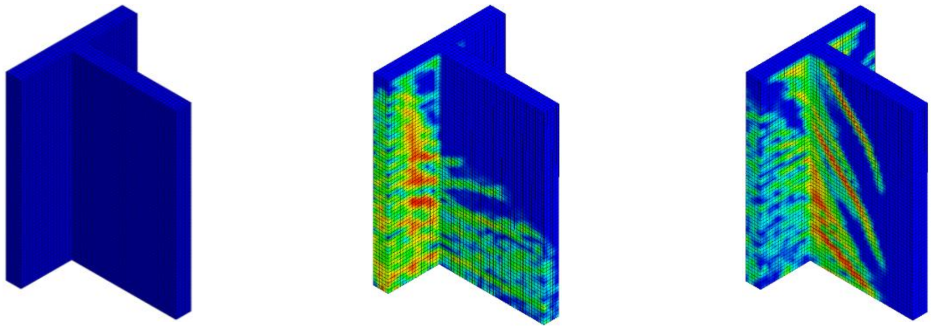

(a)Initial Condition (b)Out-of-Plane Pushover (c)In-Plane Pushover

Figure.3.2 Plastic Strain Diagram of Model of 1.5 Aspect Ratio

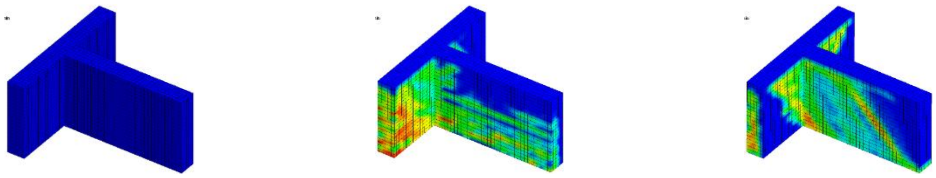

(a)Initial Condition (b)Out-of-Plane Pushover (c)In-Plane Pushover

Figure.3.3 Plastic Strain Diagram of Model of 0.5 Aspect Ratio

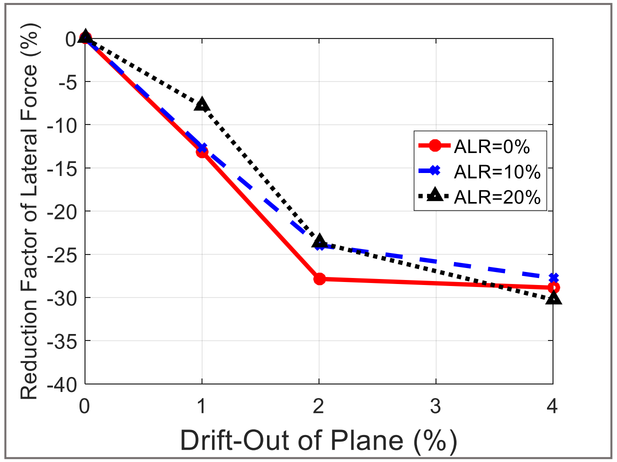


(a) T1W1H

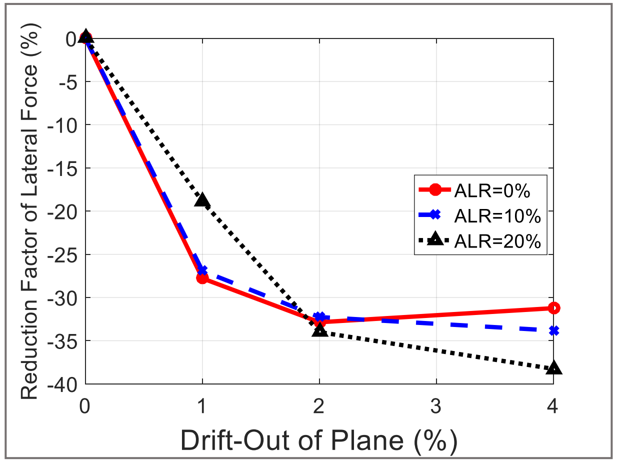


(b) T1W2H

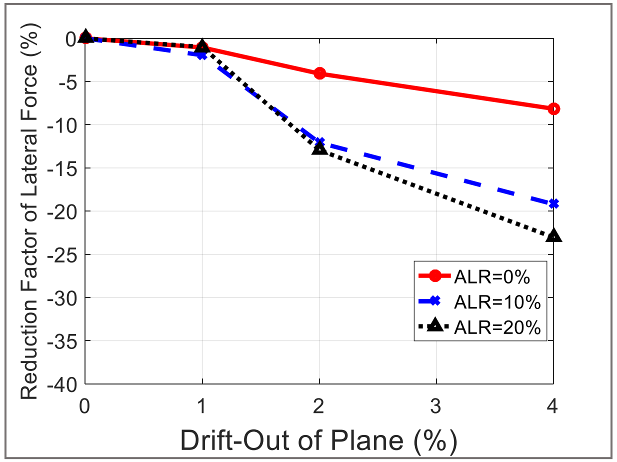


(c) T1W3H

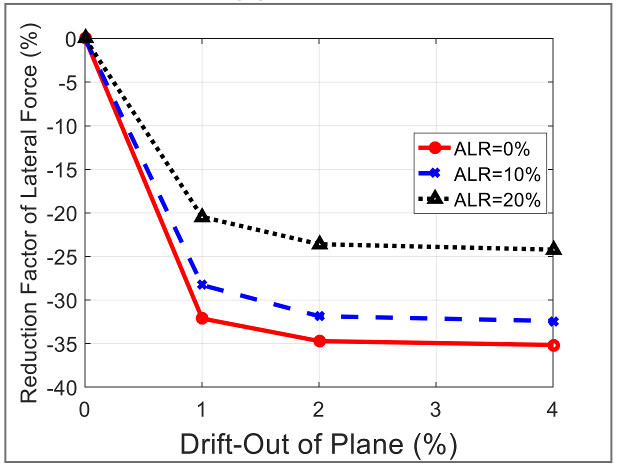


(d) T1W1M

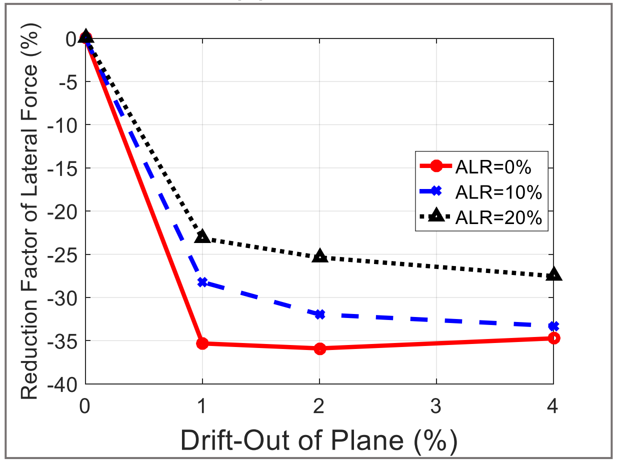


(e) T1W2M

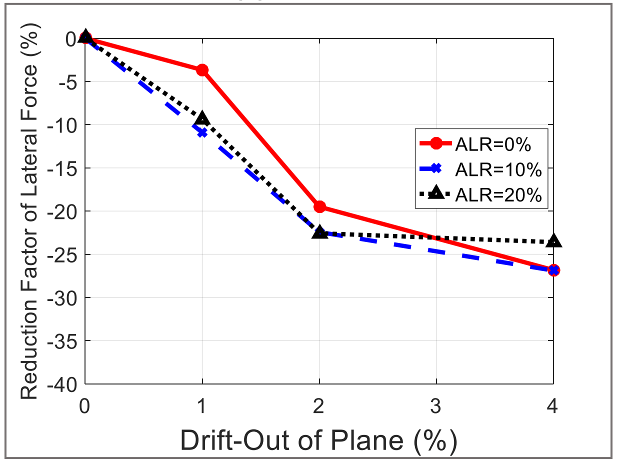


(f) T1W3M

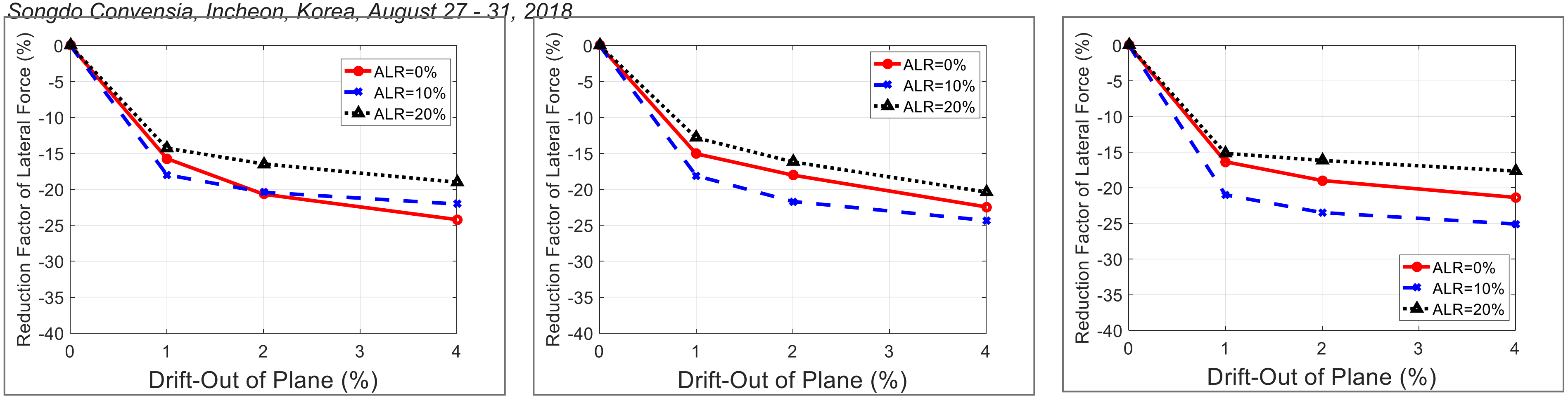


(g) T1W1L (h) T1W2L (i) T1W3L

Figure.3.4 Out-of-Plane Drift vs. Reduction Factor of Lateral Force

**REFERENCES**

C.-C. Hung, W.-T. Lu. A Performance-Based Design Method for Coupled Wall Structures. Journal of Earthquake Engineering. 21(4), pp.579-603, 2017.

C.-C. Hung, W.-T. Lu. Tall hybrid coupled structural walls: seismic behavior and design suggestions. International Journal of Civil Engineering. 2017. https://doi.org/10.1007/s40999-017-0162-2.

Wallace, J. W. (1996). Evaluation of UBC-94 provisions for seismic design of RC structural walls. Earthquake Spectra, 12(2), 327-348.

Zhang, Z., & Li, B. (2016). Seismic performance assessment of slender T-shaped reinforced concrete walls. Journal of Earthquake Engineering, 20(8), 1342-1369.

Zhang, Z., & Li, B. (2017). Seismic behaviour of non-rectangular structural RC wall in the weak axis. Magazine of Concrete Research, 69(12), 606-617.